HIGH PERFORMANCE ELECTRONIC COOLING USING NANOFLUID-AUGMENTED HEAT SINKS

by

Sarra TOUMI [a], ***Imane ALIOUANE*** [a], ***Younes MENNI*** [a,b], ***Mustafa BAYRAM*** [c*], ***Omolayo M. IKUMAPAYI*** [d], ***Abiodun BAYODE*** [d], ***Tin Tin TING*** [e,f], **and *Salih OZER*** [g]

[a] Department of Mechanical Engineering, Institute of Technology, University Center Salhi Ahmed Naama, Naama, Algeria
[b] College of Technical Engineering, National University of Science and Technology, Dhi Qar, Iraq
[c] Department of Computer Engineering, Biruni University, Istanbul, Turkey
[d] Department of Mechanical Engineering, Northwest University, Potchefstroom, South Africa
[e] Faculty of Data Science and Information Technology, INTI International University, Nilai, Malaysia
[f] School of Information Technology, UNITAR International University, Selangor, Malaysia
[g] Head of the Mechanical Engineering Department, Mus Alparslan University, Mus, Turkey

Original scientific paper
https://doi.org/10.2298/TSCI2504139T

This work examines the thermal and flow characteristics of a heat sink equipped with twisted longitudinal fins, employing a Cu-water nanofluid as the working medium. Numerical simulations, carried out using the finite element method, were used to evaluate the system's performance. The geometry is divided into three key sections: an inlet, a finned middle section subjected to a heat source, and an outlet region. Simulations covered a range of Reynolds numbers from 500-2000 and nanoparticle volume fractions, ϕ, between 0% and 4%. Analysis of the resulting temperature and velocity distributions shows that the presence of nanoparticles, along with the complex geometry of the twisted fins, leads to sharper thermal gradients and increased mixing within the fluid-flow, both of which contribute to enhanced heat transfer in the central region. Results show that increasing the Reynolds number alone enhances convective heat transfer by up to 42.8% for pure water and 36.4% for the 4% nanofluid. At a constant Re = 500, increasing the nanoparticle volume fraction from 0%-4% improves the average Nusselt number by 19.8%. When both parameters are increased simultaneously, from Re = 500 and ϕ = 0% to Re = 2000 and ϕ = 4%, the overall enhancement reaches approximately 63.4%. These findings confirm the effectiveness of the finite element method in capturing complex thermal-fluid interactions and highlight the strong potential of combining nanofluids with optimized fin geometries for advanced heat sink applications.

Key words*: heat sink, twisted fins, nanofluid, heat transfer, simulation*

Introduction

Efficient heat dissipation is a critical requirement in modern electronic, solar, and energy conversion systems, where increasing thermal loads challenge conventional cooling methods. Finned heat sinks integrated with nanofluids have garnered significant attention

* Corresponding author, e-mail: mustafabayram@biruni.edu.tr

due to their enhanced thermal conductivity, increased convective heat transfer, and improved thermal uniformity. Numerous studies have demonstrated that combining nanofluids with advanced fin geometries yields substantial thermal performance gains. Tang *et al.* [1] optimized a stepped airfoil fin micro-channel heat sink using hybrid nanofluids and machine learning, while Khatirzad and Sheikholeslami [2] examined nanofluid-cooled finned heat sinks in solar-thermoelectric hybrid systems, emphasizing energy conversion efficiency. Najafpour and Rostami [3] analyzed various fin configurations with ternary nanofluids, showing their influence on hydrothermal characteristics. Porous fin structures have also emerged as promising enhancements, as demonstrated by Abdulsahib *et al.* [4] and Suja *et al.* [5], who found improved heat transfer due to greater fluid interaction within porous domains. The geometry of the fins plays a vital role: circular [6], diamond [7], oblique [8], and bioinspired snowflake-squid shapes [9] have been extensively studied, each offering distinct thermal-hydraulic advantages. Rajangam *et al.* [10] further explored biosynthesized nanofluids in pin-fin aluminum sinks, enhancing eco-sustainability. Multi-phase Eulerian-Lagrangian models, as applied by Ambreen *et al.* [11] and Ali *et al.* [12], have enhanced the understanding of nanoparticle-fluid interactions and heat transfer characteristics in nanofluid-cooled pin-fin heat sinks, while Daiz *et al.* [13] incorporated MHD effects and thermal radiation analyze thermal management in hybrid nanofluid systems under magnetic fields. Studies by Massoudi and Hamida [14, 15] reinforced the impact of fin shape and magnetized nanofluids on heat sink efficiency. Innovative fin designs, such as staggered airfoil [16], elliptical [17], and vortex-assisted structures [18, 19], have shown significant promise in enhancing both thermal and flow performance. Meanwhile, combined passive techniques, including twisted tape with helical fins [20] and oriented pin-fin lay-outs [21], highlight the benefits of geometrical complexity.

To address thermal issues in compact electronics, this study numerically investigates a finned heat sink using Cu-water nanofluids (0%-4%) under laminar, steady-state flow. A uniform heat flux is applied to the bottom wall (finned base), and thermal performance is evaluated for Reynolds numbers between 500 and 2000 with a fixed fin twist angle of 15°, aiming to enhance cooling efficiency.

System configuration and numerical model

The study examines a 3-D finned heat sink for electronics cooling, fig. 1, consisting of a rectangular channel (0.15 m × 0.05 m × 0.03 m) and a solid aluminum base (0.1 m × 0.05 m × 0.003 m). Twenty-four aluminum twisted fins (0.0225 m × 0.02 m × $7.5 \cdot 10^{-4}$ m) with a 15° twist angle are uniformly mounted on the base, centered 0.025 m from both the inlet and outlet.

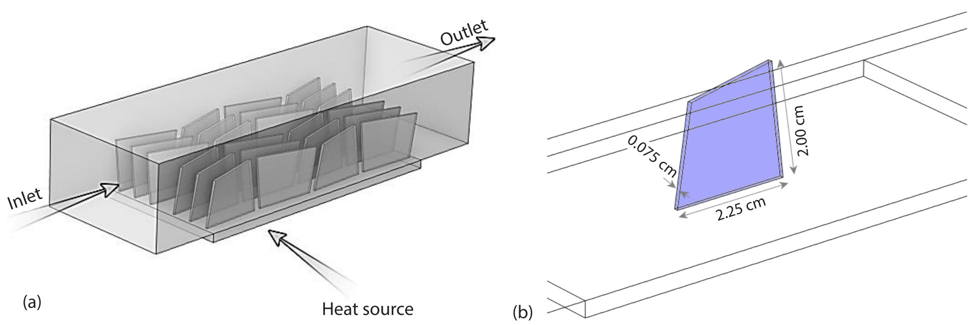

Figure 1. (a) Finned heat sink geometry and (b) twisted aluminum fin detail

The Cu-water nanofluid is modeled as laminar, incompressible, steady-state flow with 0%-4% volume concentration. Inlet conditions include uniform velocity (Re = 500-2000) and a fixed temperature of 20 °C. The outlet is at atmospheric pressure. A constant heat flux of 20000 W/m² is applied to the finned base, with adiabatic walls and no-slip, impermeable boundaries. Thermophysical properties of water and Cu are taken from [22]. The flow and thermal behavior are governed by the 3-D continuity, momentum, and energy equations, expressed, respectively:

$$\nabla \vec{u} = 0 \tag{1}$$

$$\rho_{\text{nf}} \left(\vec{u} \nabla \right) \vec{u} = -\nabla p + \mu_{\text{nf}} \nabla^2 \vec{u} \tag{2}$$

$$\rho_{\text{nf}} C_{p,\text{nf}} \left(\vec{u} \nabla \right) T = k_{\text{nf}} \nabla^2 T \tag{3}$$

where $\vec{u}$ is the velocity vector, p – the pressure, and T – the temperature. The effective thermophysical properties of the Cu-water nanofluid (density, ρ_{nf}, viscosity, μ_{nf}, specific heat capacity, $C_{p,\text{nf}}$, and conductivity, k_{nf}) are calculated using standard correlations [23, 24]:

$$\rho_{\text{nf}} = \left(1 - \phi \right) \rho_{\text{bf}} + \phi \rho_{\text{np}} \tag{4}$$

$$\mu_{\text{nf}} = \frac{\mu_{\text{bf}}}{\left(1 - \phi \right)^{2,5}} \tag{5}$$

$$C_{p,\text{nf}} = \left(1 - \phi \right) C_{p,\text{bf}} + \phi C_{p,\text{np}} \tag{6}$$

$$k_{\text{nf}} = \frac{k_{\text{np}} + 2k_{\text{bf}} + 2\phi \left(k_{\text{np}} - k_{\text{bf}} \right)}{k_{\text{np}} + 2k_{\text{bf}} - \phi \left(k_{\text{np}} - k_{\text{bf}} \right)} k_{\text{bf}} \tag{7}$$

where ϕ is the volume fraction of nanoparticles, while the subscripts nf, bf, and np correspond to the nanofluid, base fluid, and nanoparticles, respectively. A high quality unstructured mesh is shown in fig. 2 and was generated for finite element analysis. It consists of 1260014 elements and 247309 nodes, including tetrahedra, prisms, pyramids, and surface elements. The total mesh volume is 240 cm³, with a minimum element quality of 0.07334 and an average quality of 0.6938, ensuring sufficient accuracy and numerical stability.

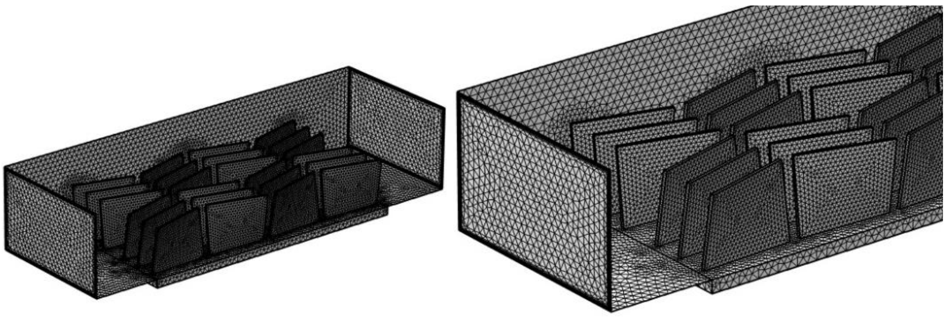

Figure 2. The 3-D unstructured mesh of the finned heat sink

Model validation was performed by comparing the simulated temperature distribution along the fin with the results of Chen *et al.* [25], who employed an inverse method with experimental data to assess heat transfer in a plate-fin heat sink. A fin spacing of 0.005 m was used for comparison, and the present results showed good agreement, confirming the reliability of the numerical model under similar thermal and flow conditions, as illustrated in fig. 3.

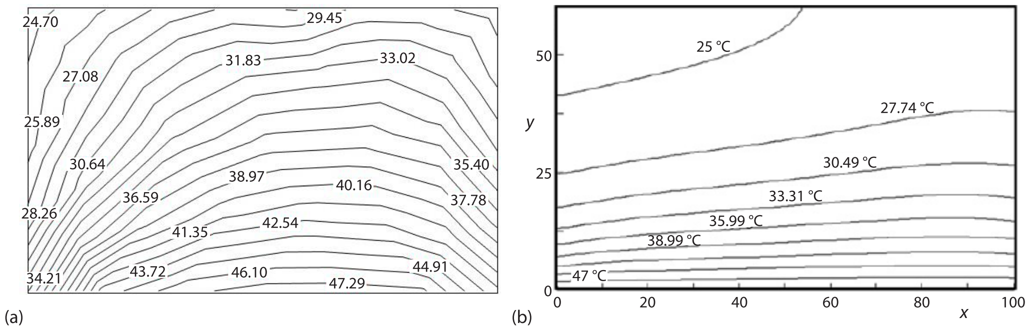

Figure 3. Validation of simulated fin temperature with data from [25]

Results and analysis

Figure 4 illustrates the velocity magnitude distributions within the simulated twisted longitudinal finned heat sink at a fixed Cu-water nanoparticle volume fraction of 4%, for Reynolds numbers of 500, 1000, and 1500. The velocity field exhibits distinct characteristics across

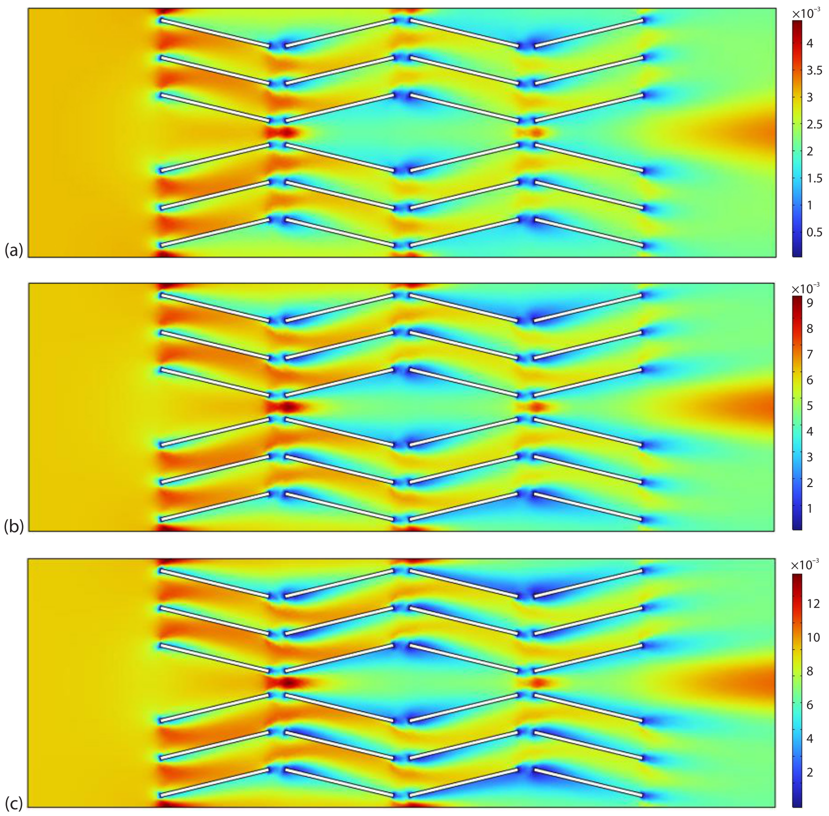

Figure 4. Velocity magnitude at 4% volume fraction for varying Renolds numbers; (a) Re = 500, (b) Re = 1000, and (c) Re = 1500

the three defined regions of the heat sink, strongly influenced by both the internal geometry and the flow regime.

In the inlet zone (Region 1), where the channel is smooth, the flow begins to develop from an initially uniform profile into a more parabolic shape, with velocity gradients forming near the walls due to viscous effects. In the central finned zone (Region 2), the introduction of twisted longitudinal fins dramatically alters the flow dynamics. The fins induce secondary flows, local accelerations, and recirculating structures that disrupt the symmetry of the velocity field. These effects become more pronounced with increasing Reynolds number, indicating enhanced turbulence and mixing. Finally, in the outlet zone (Region 3), where the geometry returns to a smooth, the velocity profile gradually stabilizes. However, remnants of the disturbed flow patterns persist, especially at higher Reynolds numbers, reflecting the strong influence of the upstream finned region.

Figure 5 illustrates the temperature contours at a fixed Reynolds number of 500 for varying Cu-water nanoparticle volume fractions (0%, 2%, and 4%) across the three regions of the heat sink. In the inlet region, where no heat is applied, the temperature remains uniform and low for all volume fractions, with minimal thermal activity, primarily due to the direction of flow bringing in cooler fluid before it reaches the heated finned region. As the fluid enters the finned and heated region, clear differences emerge based on the nanoparticle concentration. At

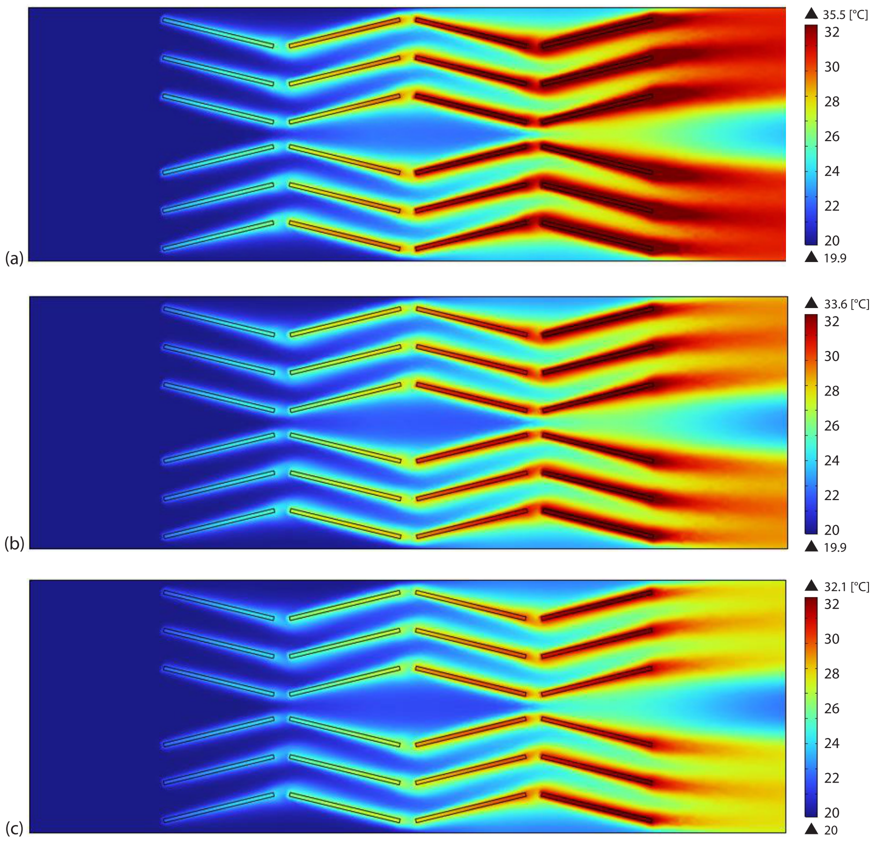

Figure 5. Temperature contours at Re = 500 for various volume fractions numbers; (a) ϕ = 0%, (b) ϕ = 2%, and (c) ϕ = 4%

0% volume fraction (pure water), the temperature builds up significantly along the heated base, with wide, diffused contours indicating weak convective transport and slow thermal diffusion. The heat remains concentrated near the wall, and the thermal boundary-layer is thick. With 2% nanoparticle addition, the contours become more compressed, and the fluid temperature decreases more rapidly along the flow direction. This reflects improved heat conduction and enhanced convection due to the presence of Cu nanoparticles. At 4% volume fraction, the effect is even more pronounced: the thermal boundary-layer becomes thinner, the contours are denser near the heated surface, and the temperature drop along the flow is more significant. The nanofluid at this concentration shows superior thermal performance, aided by both its high thermal conductivity and the mixing effects induced by the twisted fins. In the outlet region, the fluid exits with lower temperatures as the volume fraction increases, demonstrating that more heat has been successfully extracted in the upstream region. Overall, fig. 5 confirms that increasing the nanoparticle concentration enhances heat transfer throughout all regions of the heat sink, especially in the finned section where thermal gradients are highest.

Figure 6 illustrates the outlet surface temperature distributions in Region 3 of the heat sink for a fixed Cu-water nanoparticle volume fraction of 4%, considering three different Reynolds numbers, 500, 1000, and 1500. The results clearly demonstrate that the outlet temperature decreases as the Reynolds number increases, reflecting enhanced convective heat transfer at higher flow rates. At Re = 500, the outlet surface retains relatively high temperatures, indicating that the fluid has extracted less heat from the heated finned region due to slower velocity and weaker convective transport. As the Reynolds number increases to 1000, the outlet temperature drops noticeably, showing improved heat removal as the fluid moves faster and absorbs more thermal energy along the flow path. At Re = 1500, the outlet surface temperature reaches its lowest level, signifying optimal cooling performance. The increased velocity promotes stronger mixing and more efficient thermal energy transport, allowing the nanofluid to carry away heat more effectively before reaching the outlet. This trend confirms that higher Reynolds numbers, when combined with the enhanced thermal conductivity of the 4% Cu-water nanofluid, significantly improve heat dissipation in the final region of the heat sink.

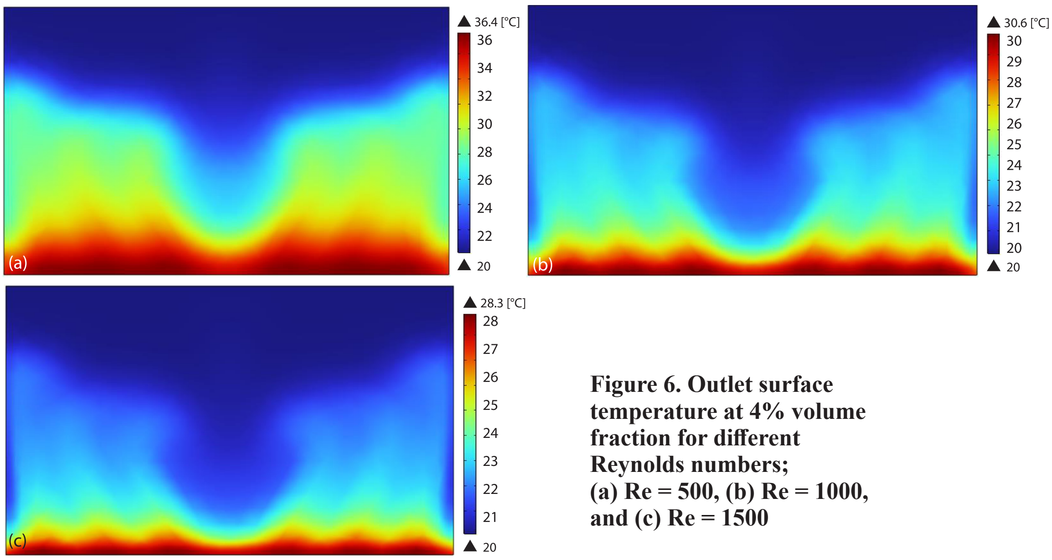

Figure 6. Outlet surface temperature at 4% volume fraction for different Reynolds numbers; (a) Re = 500, (b) Re = 1000, and (c) Re = 1500

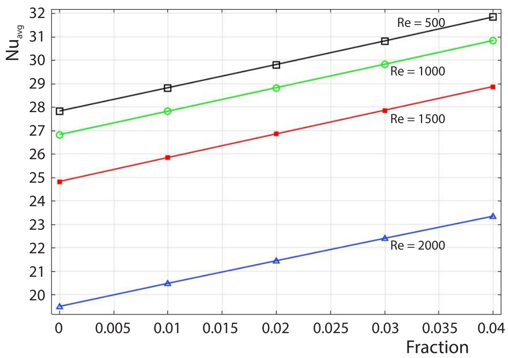

Table 7. Thermal performance in terms of Nusselt number for various Reynolds and volume fractions

Figure 7 illustrates how the average Nusselt number varies with different fractions (0% to 4%) and Reynolds numbers (500-2000), demonstrating the influence of both flow intensity and nanoparticle loading on convective heat transfer. The data reveal a clear upward trend in Nusselt number as either the Reynolds number or the volume fraction increases. At constant Reynolds numbers, the inclusion of Cu nanoparticles significantly improves the heat transfer capability of the fluid by enhancing its thermal conductivity. For instance, when Reynolds number is fixed at 500, introducing 4% nanoparticles raises the Nusselt number from 19.492 (pure water) to 23.343 (at ϕ = 4%), marking a gain of about 19.8%. Similar improvements are observed at higher flow rates, with a 16.3% increase at Re = 1000 and a 14.4% rise at Re = 2000. These results confirm the positive impact of nanofluid concentration on thermal performance, particularly under laminar to transitional flow regimes. Similarly, for a fixed volume fraction, increasing the Reynolds number leads to a marked rise in Nusselt number due to stronger convective transport and thinner thermal boundary-layers. For instance, at 0% volume fraction, Nusselt number rises from 19.492-27.832, a 42.8% increase, while at 4%, it rises from 23.343-31.847, representing a 36.4% enhancement. The most substantial overall improvement occurs at ϕ = 4% and Re = 2000, with a Nusselt number of 31.847, which is approximately 63.4% higher than the baseline case of ϕ = 0% and Re = 500. These results clearly demonstrate that both increasing nanoparticle concentration and flow rate significantly improve the convective heat transfer capability of the finned heat sink.

Conclusions

This research has demonstrated the strong potential of twisted longitudinal finned heat sinks combined with Cu-water nanofluids for enhanced thermal performance. By exploring a range of Reynolds numbers and nanoparticle volume fractions, it was found that both parameters play a critical role in improving convective heat transfer. The addition of Cu nanoparticles led to a noticeable increase in thermal conductivity and heat removal efficiency, with the most pronounced benefits observed at higher concentrations and flow rates. The twisted fin geometry contributed significantly to the disruption of boundary-layers and the promotion of secondary flows, further improving heat transfer across the heated surface.

The velocity and temperature fields confirmed the influence of these design enhancements across all three regions of the heat sink, particularly within the finned zone where heat transfer was most intense. Importantly, the combination of high Reynolds numbers and a ϕ of 4% yielded the best performance, increasing the Nusselt number by over 63% compared to the baseline case.

Overall, the integration of nanofluids and optimized fin geometries presents a promising strategy for advancing the efficiency of heat exchangers in electronics cooling, solar thermal systems, and other compact high heat flux applications. Future studies may extend this work to transient conditions, different fin configurations, and alternative nanoparticle materials to further broaden its applicability.

References

[1] Tang, Z., *et al*., Multi-Objective Optimization of a Hybrid Nanofluid Jet Impingement Micro-Channel Heat Sink With Stepped Airfoil Fins Based on Machine Learning, *Engineering Analysis with Boundary Elements*, *179* (2025), 106380
[2] Khatirzad, H., Sheikholeslami, M., Numerical Investigation of Hybrid Nanofluid-Flow in a Finned Heat Sink Integrated with a Concentrated Solar System and Thermoelectric Generator, *Renewable Energy*, *245* (2025), 122783
[3] Najafpour, A., Rostami, M. H., Numerical Analysis of Thermal and Hydrothermal Characteristics of a Heat Sink with Various Fin Configurations and Ternary Nanofluid Composition, *Case Studies in Thermal Engineering*, *68* (2025), 105928
[4] Abdulsahib, A. D., *et al.*, Optimizing Heat Sink Performance by Replacing Fins from Solid to Porous inside Various Enclosures Filled with a Hybrid Nanofluid, *Frontiers in Heat and Mass Transfer*, *22* (2024), 6, pp. 1777-1804
[5] Suja, S. B., *et al.*, Numerical Investigation of Thermal and Hydraulic Characteristics in Porous Pin Fin Heat Sinks Using Single Phase Nanofluids, *International Journal of Thermofluids*, *22* (2024), 100677
[6] Basem, A., *et al.*, Exploring the Efficiency of Employing Fe_3O_4-MWCNT Nanofluids in a Heat Sink Equipped with Circular Micro Pin-Fins, *International Journal of Thermofluids*, *24* (2024), 100928
[7] Duangthongsuk, W., *et al*., Experimental Study on the Hydrothermal Performance of Nanofluids-Cooled Heat Sinks with Diamond Shape Micro Pin-Fin Structures, *International Journal of Thermofluids*, *22* (2024), 100691
[8] Tiwary, B., *et al*., Thermofluidic Characteristic of a Nanofluid-Cooled Oblique Fin Heat Sink: An Experimental and Numerical Investigation, *International Journal of Thermal Sciences*, *171* (2022), 107214
[9] Yue, L., *et al*., Cooling Characteristics of Nanofluids in a Snowflake and Squid Fin Composite Bionic Micro-Channel Heat Sink, Colloids and Surfaces A: *Physicochemical and Engineering Aspects*, *705* (2025), 135614
[10] Rajangam, V., *et al*., Hydrodynamics and Heat Transfer Characteristics of Biosynthesized SiC-Alkaline Water and ZnO-Alkaline Water Nanofluids in an Aluminum Plate Pin-Fin Heat Sink, *Desalination and Water Treatment*, *307* (2023), Sept., pp. 232-250
[11] Ambreen, T., *et al*., Irreversibility and Hydrothermal Analysis of the MWCNT/GNPs-Based Nanofluids for Electronics Cooling Applications of the Pin-Fin Heat Sinks: Multi-Phase Eulerian-Lagrangian Modelling, *Case Studies in Thermal Engineering*, *31* (2022), 101806
[12] Ali, N. B., *et al*., Eulerian-Lagrangian Numerical Investigation of the Fluid-Flow Properties and Heat Transfer of a Nanofluid-Cooled Micro Pin-Fin Heat Sink, *Journal of the Taiwan Institute of Chemical Engineers*, *164* (2024), 105674
[13] Daiz, A., *et al*., Thermal Management of Pin-Fin Heat Sinks in Square Vented Cavity Using Magnetohydrodynamic Hybrid Nanofluids under Thermal Radiation, *International Communications in Heat and Mass Transfer*, *162* (2025), 108568
[14] Massoudi, M. D., Hamida, M. B. B., Combined Impacts of Square Fins Fitted Wavy Wings and Micropolar Magnetized-Radiative Nanofluid on the Heat Sink Performance, *Journal of Magnetism and Magnetic Materials*, *574* (2023), 170655
[15] Massoudi, M. D., *et al*., The Influence of Multiple Fins Arrangement Cases on Heat Sink Efficiency of MHD MWCNT-Water Nanofluid Within Tilted T-Shaped Cavity Packed with Trapezoidal Fins Considering Thermal Emission Impact, *International Communications in Heat and Mass Transfer*, *126* (2021), 105468
[16] Babar, H., *et al.*, Staggered Oriented Airfoil Shaped Pin-Fin Heat Sink: Investigating the Efficacy of Novel Water Based Ferric Oxide-Silica Hybrid Nanofluid, *International Journal of Heat and Mass Transfer*, *194* (2022), 123085
[17] Bahiraei, M., *et al*., Employing Elliptical Pin-Fins and Nanofluid Within a Heat Sink for Cooling of Electronic Chips Regarding Energy Efficiency Perspective, *Applied Thermal Engineering*, *183* (2021), 116159
[18] Gonzalez, A., *et al*., Numerical Study of the Fluid Dynamics and Heat Transfer for Shear-Thinning Nanofluids in a Micro Pin-Fin Heat Sink, *Case Studies in Thermal Engineering*, *28* (2021), 101635
[19] Aguirre, I., *et al*., Numerical Study on the Use of Shear-Thinning Nanofluids in a Micro Pin-Fin Heat Sink Including Vortex Generators and Changes in Pin Shapes, *Journal of the Taiwan Institute of Chemical Engineers, 136* (2022), 104400

[20] Jafaryar, M., *et al*., Hybrid Nanofluid Turbulent Transportation through a Tube with an Innovative Twisted Tape Combined with Helical Fins Heat Sink, *Sustainable Energy Technologies and Assessments*, *53* (2022), 102702
[21] Nawaz, S., *et al*., Oriented Square Shaped Pin-Fin Heat Sink: Performance Evaluation Employing Mixture Based on Ethylene Glycol/Water Graphene Oxide Nanofluid, *Applied Thermal Engineering*, *206* (2022), 118085
[22] Hissouf, M., *et al*., Numerical Study of a Covered Photovoltaic-Thermal Collector (PVT) Enhancement Using Nanofluids, *Solar Energy*, *199* (2020), Mar., pp. 115-127
[23] Brinkman, H. C., The Viscosity of Concentrated Suspensions and Solutions, *Journal of Chemical Physics*, 20 (1952), 4, pp. 571-571
[24] Hamilton, R. L., Crosser, O. K., Thermal Conductivity of Heterogeneous Two-Component Systems, *Industrial & Engineering Chemistry Fundamentals*, *1* (1962), 3, pp. 187-191
[25] Chen, H. T., *et al*., Investigation of Heat Transfer Characteristics In Plate-Fin Heat Sink, *Applied Thermal Engineering*, *50* (2013), 1, pp. 352-360

Paper submitted: March 2, 2025
Paper revised: May 10, 2025
Paper accepted: June 28, 2025